

A Fast Vector Potential Method Using Tangentially Continuous Vector Finite Elements

Romanus Dyczij-Edlinger¹, Guanghua Peng¹, Jin-Fa Lee²

Romanus Dyczij-Edlinger

Motorola CCRL

Maildrop IL02-EA901

1301 E. Algonquin Rd.

Schaumburg, IL 60196, U.S.A.

FAX: (847) 538-4713

E-mail: are003@email.mot.com

Abstract

An efficient finite element method for driven time-harmonic wave propagation problems is proposed. The special properties of tangentially continuous vector finite elements (TVFEMs) are utilized to formulate an ungauged vector potential scheme in terms of the field method plus one very sparse “gradient matrix” with two non-zero integer or pointer entries per row. The suggested formalism is intended for use with iterative solvers. It combines the simplicity and modest memory requirements of the field formulation with the superior numerical convergence of the ungauged vector potential scheme.

I. INTRODUCTION

To formulate a driven wave propagation problem with TVFEMs, two approaches are usually considered: the field formulation (in \vec{E} or \vec{H}) and the vector potential approach (in $\vec{A} - V$ or $\vec{T} - \psi$, respectively). Which scheme is preferable, depends on whether the resulting equation

¹R. Dyczij-Edlinger and G. Peng are with Motorola CCRL, IL02-EA901, Schaumburg, IL 60195-1078, USA.

²J.-F. Lee is with ECE Dept. Worcester Polytechnic Institute, 100 Institute Rd., Worcester, MA 01609, USA.

³This work was supported by Motorola Inc.

systems are solved by direct or iterative methods. As long as the number of unknowns is in the low ten thousands, the memory and CPU time expenses for direct solvers are quite acceptable. In these cases, the \vec{E} formulation is the method of choice.

However, practical applications often involve structures that are electrically large, highly inhomogeneous, or very complicated in shape. For such configurations, large numbers of unknowns are unavoidable, and the computational costs of complete matrix factorizations may become prohibitively high. It has turned out [1] that the \vec{E} formulation does not lend itself very well to efficient iterative solvers such as the preconditioned conjugate gradient (PCG) method. Fortunately, the ungauged $\vec{A}-V$ formulation has proven to converge much better [2] [3]; a fact that has also been verified in an eddy current context. [4]. A major reason for the unequal convergence characteristics of the \vec{E} and $\vec{A}-V$ schemes was pointed out in [3].

One obvious disadvantage of the $\vec{A}-V$ method is that the augmented scalar potential almost doubles the number of non-zero entries in the system matrix [3], which leads to nearly twice as many floating point operations (FLOPs) per iteration step as the \vec{E} formulation. With regard to the computer implementation, it is also unsatisfactory that the $\vec{A}-V$ approach requires several new types of volume and surface integrals (for scalar-scalar and scalar-vector interactions), although its solution space for the electric field remains just the same as that of the basic \vec{E} scheme on the same mesh.

In this paper, we propose an improved $\vec{A}-V$ formulation that overcomes much of the overhead mentioned above. The new approach decreases memory consumption and per-iteration-FLOPs to levels very similar to the \vec{E} scheme, while maintaining the fast convergence rates of the original method. The key step in our formulation is an index representation of the gradient operator in discretized space which does not require the explicit storage of any matrix entries involving

the scalar potential. The associated (sub-)matrix-times-vector multiplications get bypassed by a moderate number of additions/subtractions, and the system matrix and right hand side (RHS) vector reduce to those of the \vec{E} formulation. Overall, the implementation of the simplified $\vec{A} - V$ scheme just requires an additional “gradient matrix” with two index or pointer entries per row and some modifications in the PCG solver.

The remainder of this paper is organized as follows: In *Section II*, we give a short review of the \vec{E} and $\vec{A} - V$ formulations, investigate the close relationship between both schemes and introduce the gradient matrix [G]. These findings are used in *Section III* to construct an efficient solver. *Section IV* presents some numerical examples which demonstrate the efficiency of the suggested approach.

II. THEORY

We consider a time-harmonic boundary value problem (BVP) for the vector wave equation,

$$\nabla \times ([\mu_r]^{-1} \nabla \times \vec{E}) - k_0^2 [\epsilon_r] \vec{E} = \vec{0} \quad \text{in } \Omega, \quad (1)$$

$$\vec{H} \times \vec{n} = \vec{H}_t \quad \text{given on } \Gamma_H, \quad (2)$$

$$\vec{E} \times \vec{n} = \vec{0} \quad \text{given on } \Gamma_E = \Gamma - \Gamma_H. \quad (3)$$

where Ω is a finite, three dimensional domain with boundary Γ and outward normal vector \vec{n} , ϵ_r and μ_r stand for the relative permittivity and permeability, and k_0 and η_0 for the free space wavenumber and characteristic impedance, respectively. The boundary condition (3) has been chosen homogeneous to simplify notation later on.

A. \vec{E} Formulation

In the discretization process, a TVFEM approach for the electric field,

$$\vec{E} = \sum e_i \vec{W}_i, \quad (4)$$

with basis functions \vec{W}_i , is plugged into the associated weak form of the BVP (1)-(3). The resulting set of Galerkin equations for the unknown coefficient vector, $\vec{x}_E = \text{col}(e_i)$, can be written as

$$[M_{EE}] \cdot \vec{x}_E = \vec{r}_E, \quad (5)$$

where

$$[M_{EE}]_{ij} = \int_{\Omega} \left\{ (\nabla \times \vec{W}_i) \cdot [\mu_r]^{-1} (\nabla \times \vec{W}_j) - k_0^2 \vec{W}_i \cdot [\epsilon_r] \vec{W}_j \right\} d\Omega, \quad (6)$$

$$\vec{r}_{E,i} = -jk_0\eta_0 \int_{\Gamma_H} \vec{W}_i \cdot (\vec{H}_t \times \vec{n}) d\Gamma \quad (7)$$

B. $\vec{A} - V$ Formulation

Our formulation is based on a time-integrated vector potential \vec{A} and an electric scalar potential V given by

$$\vec{A}: \quad \nabla \times \vec{A} = -j\omega \vec{B}, \quad (8)$$

$$V: \quad \vec{A} + \nabla V = \vec{E}. \quad (9)$$

Now, the BVP (1)-(3) can be stated as

$$\nabla \times ([\mu_r]^{-1} \nabla \times \vec{A}) - k_0^2 [\epsilon_r] (\vec{A} + \nabla V) = \vec{0} \quad \text{in } \Omega, \quad (10)$$

$$([\mu_r]^{-1} \nabla \times \vec{A}) \times \vec{n} = -jk_0\eta_0 \vec{H}_t \times \vec{n} \quad \text{on } \Gamma_H, \quad (11)$$

$$\left. \begin{aligned} \vec{A} \times \vec{n} &= \vec{0} \\ V &= 0 \end{aligned} \right\} \quad \text{on } \Gamma_E. \quad (12)$$

Note that (10)-(12) uniquely define \vec{E} , while still allowing for gauge transformations between solution pairs (\vec{A}_1, V_1) and (\vec{A}_2, V_2) of the form:

$$\phi \in H_0^1(\Omega; \Gamma_E), \quad \vec{A}_2 = \vec{A}_1 + \nabla \phi, \quad (13)$$

$$V_2 = V_1 - \phi. \quad (14)$$

Gauged versions can be found in [5] [6] [7], but will not be considered here. To obtain a set of finite element equations, we expand the potentials by

$$\vec{A} = \sum a_i \vec{W}_i \quad \text{and} \quad V = \sum \varphi_k \xi_k, \quad (15)$$

where \vec{W}_i and ξ_k stand for vector and scalar basis functions, respectively, and apply a Galerkin process to (10)-(12):

$$\begin{aligned} \forall W_i : \quad & \int_{\Omega} \left[(\nabla \times \vec{W}_i) \cdot [\mu_r]^{-1} (\nabla \times \vec{A}) - k_0^2 \vec{W}_i \cdot [\epsilon_r] (\vec{A} + \nabla V) \right] d\Omega = \\ & -jk_0\eta_0 \int_{\Gamma} \vec{W}_i \cdot (\vec{H}_t \times \vec{n}) d\Gamma \end{aligned} \quad (16)$$

$$\forall \nabla \xi_k : \quad -k_0^2 \int_{\Omega} \nabla \xi_k \cdot [\epsilon_r] (\vec{A} + \nabla V) d\Omega = -jk_0\eta_0 \int_{\Gamma_H} \nabla \xi_k \cdot (\vec{H}_t \times \vec{n}) d\Gamma \quad (17)$$

Note that the weighting functions are chosen from $\{\vec{W}_i\} \cup \{\nabla \xi_k\}$. In matrix form, (16) and (17) read

$$\begin{bmatrix} M_{AA} & M_{AV} \\ M_{AV}^T & M_{VV} \end{bmatrix} \begin{bmatrix} \vec{x}_A \\ \vec{x}_V \end{bmatrix} = \begin{bmatrix} \vec{r}_A \\ \vec{r}_V \end{bmatrix}, \quad (18)$$

where $\vec{x}_A = \text{col}(a_i)$ and $\vec{x}_V = \text{col}(\varphi_k)$ are the coefficient vectors associated with \vec{A} and V , respectively, and

$$[M_{AA}] = [M_{EE}], \quad (19)$$

$$\vec{r}_A = \vec{r}_E, \quad (20)$$

$$\vec{r}_{V,k} = -jk_0\eta_0 \int_{\Gamma_H} \nabla \xi_k \cdot (\vec{H}_t \times \vec{n}) d\Gamma, \quad (21)$$

$$[M_{AV}]_{ik} = -k_0^2 \int_{\Omega} \vec{W}_i \cdot [\epsilon_r] \nabla \xi_k d\Omega, \quad (22)$$

$$[M_{VV}]_{kl} = -k_0^2 \int_{\Omega} \nabla \xi_k \cdot [\epsilon_r] \nabla \xi_l d\Omega. \quad (23)$$

C. Relating the $\vec{A} - V$ to the \vec{E} formulation

As pointed out in [3], the primary goal of the ungauged $\vec{A} - V$ formulation is to provide an alternative basis $\{\xi_k\}$ for all gradients in $\mathcal{V} := \text{span}\{\vec{W}_i\}$, which is then utilized to improve numeric convergence. Thus, we request

$$\left\{ \vec{E} \in \mathcal{V} \mid \vec{E} = \nabla \phi, \phi \in H_0^1(\Omega; \Gamma_E) \right\} \subseteq \left\{ \nabla V, V \in \text{span}\{\xi_k\} \right\}. \quad (24)$$

The most natural way of defining the basis $\{\xi_k\}$ is implied by the construction of TVFEM spaces themselves: Just add the associated set of nodal basis functions [8] [9]: linear functions for edge elements, quadratics for $H_1(\text{curl})$, etc. This procedure even yields the scalar space of smallest dimension possible:

$$\left\{ \vec{E} \in \mathcal{V} \mid \vec{E} = \nabla \phi, \phi \in H_0^1(\Omega; \Gamma_E) \right\} = \left\{ \nabla V, V \in \text{span}\{\xi_k\} \right\}, \quad (25)$$

$$\dim \text{span}\{\nabla \xi_k\} = \dim \text{span}\{\xi_k\} = K, \quad (26)$$

where K is the number of free nodes. From (25) and (9), it is clear that the augmented scalar unknowns do not enlarge the solution space for \vec{E} . Instead, the Galerkin equations (16) and (17) allow for K linear independent gauge transformations (14), and the system matrix in (18) becomes singular with rank deficiency K . The fact that the nodal basis functions do not add any new information to the system suggests that there might be a way to formulate (18) without actually constructing $[M_{AV}]$ and $[M_{VV}]$. In the following, we will present the solution for edge elements only.

Due to equality in (25), every gradient in $\text{span}\{\nabla\xi_k\}$ can also be expressed in terms of edge element basis functions. For the associated coefficient vectors, $\vec{e} = \text{col}(e_i)$ and $\vec{\phi} = \text{col}(\phi_k)$, this relation may be written as an $I \times K$ matrix $[G]$ representing the gradient operator in discretized space:

$$[G] : \vec{\phi} \rightarrow \vec{e}(\vec{\phi}) : \quad \vec{e}(\vec{\phi}) = [G] \cdot \vec{\phi}. \quad (27)$$

To identify the elements of the “gradient matrix” $[G]$, we consider a vector basis function \vec{W}_i defined along edge $\{mn\}$ from node m to node n . We have [8] [9]

$$\int_{\text{edge}} \vec{W}_i \cdot d\vec{l} = \begin{cases} 1 & \text{along edge } \{mn\}, \\ 0 & \text{along all other edges.} \end{cases} \quad (28)$$

The line integral along edge $\{mn\}$ of a gradient field, $\vec{E} = \nabla\phi \in \mathcal{V}$ yields

$$\begin{aligned} \int_m^n \vec{E} \cdot d\vec{l} &= \underbrace{\int_m^n e_i \vec{W}_i \cdot d\vec{l}}_{e_i} = \underbrace{\int_m^n \nabla\phi \cdot d\vec{l}}_{\phi_n - \phi_m} \\ &= e_i = \phi_n - \phi_m, \end{aligned} \quad (29)$$

i.e., the edge coefficient e_i is uniquely defined by the difference of the nodal coefficients associated with the starting and ending point, respectively. Thus, the gradient matrix has two and only two non-zero entries per row, namely

$$[G]_{im} = -1 \quad \text{and} \quad [G]_{in} = +1. \quad (30)$$

We now have an efficient way to state (9) in terms of finite element coefficients:

$$e_{i\{mn\}} = a_{i\{mn\}} + \phi_n - \phi_m \quad (31)$$

and, in matrix form,

$$\vec{x}_E = \begin{bmatrix} I & G \end{bmatrix} \cdot \begin{bmatrix} \vec{x}_A \\ \vec{x}_V \end{bmatrix}. \quad (32)$$

This result justifies our somewhat unusual definition of the potentials in (8) and (9). Since (32) will be evaluated in each PCG iteration step, this equation ought to be kept as simple as possible.

Since both sets of Galerkin equations, (16) and (17), are actually in terms of \vec{E} only, we may use (32) to simplify the equation system (18). For its first row, we get immediately

$$[M_{EE}] \cdot \begin{bmatrix} I & G \end{bmatrix} \cdot \begin{bmatrix} \vec{x}_A \\ \vec{x}_V \end{bmatrix} = \vec{r}_E. \quad (33)$$

If we now replace the gradient weights in the Galerkin equations (17) by their edge element representations, the second row of (18) yields

$$[G]^T \cdot [M_{EE}] \cdot \begin{bmatrix} I & G \end{bmatrix} \cdot \begin{bmatrix} \vec{x}_A \\ \vec{x}_V \end{bmatrix} = [G]^T \cdot \vec{r}_E. \quad (34)$$

Finally, by combining (33) and (34), the matrix and RHS become

$$\begin{bmatrix} M_{AA} & M_{AV} \\ M_{AV}^T & M_{VV} \end{bmatrix} = \begin{bmatrix} I & G \end{bmatrix}^T \cdot [M_{EE}] \cdot \begin{bmatrix} I & G \end{bmatrix}, \quad (35)$$

$$\begin{bmatrix} \vec{r}_A \\ \vec{r}_V \end{bmatrix} = \begin{bmatrix} I & G \end{bmatrix}^T \cdot \vec{r}_E, \quad (36)$$

$$(37)$$

and, for the complete matrix equation of the ungauged $\vec{A} - V$ scheme, we get

$$\begin{bmatrix} I & G \end{bmatrix}^T \cdot [M_{EE}] \cdot \begin{bmatrix} I & G \end{bmatrix} \cdot \begin{bmatrix} \vec{x}_A \\ \vec{x}_V \end{bmatrix} = \begin{bmatrix} I & G \end{bmatrix}^T \cdot \vec{r}_E. \quad (38)$$

III. COMPUTER IMPLEMENTATION

A. Matrix Representation

The conventional $\vec{A} - V$ approach requires the explicit construction of the matrices $[M_{VV}]$ and $[M_{AV}]$. Since each row of $[M_{AV}]$ couples the corresponding edge to all nodes of the adjacent elements, the memory requirements for this matrix are very high. (We remark that $[M_{VV}]$ is far cheaper.) As a result, the potential method may lead to almost twice as many non-zero matrix entries as the field formulation (see TABLE I).

The present approach implements the ungauged $\vec{A} - V$ method in terms of the \vec{E} scheme plus one gradient matrix $[G]$. Since $[G]$ is given by just $2K$ indices or pointers, the additional memory requirements are very moderate.

B. Iterative Solver

Since the equations derived in *Section III* do not impose any restrictions on the material properties, the formalism fully covers the anisotropic case. For simplicity, however, we will assume in the following that $[M_{EE}]$ be symmetric and focus on the PCG method only [10]. A detailed analysis of preconditioners for singular systems can be found in [11] [12].

Our implementation uses either diagonal scaling or incomplete Cholesky decomposition as preconditioner. In the latter case, we compute and factorize $[M_{VV}]$ explicitly, but neglect the expensive coupling matrix $[M_{AV}]$:

$$\begin{bmatrix} M_{AA} & M_{AV} \\ M_{VA} & M_{VV} \end{bmatrix} \approx \begin{bmatrix} L_{AA} & 0 \\ 0 & L_{VV} \end{bmatrix} \cdot \begin{bmatrix} L_{AA} & 0 \\ 0 & L_{VV} \end{bmatrix}^T, \quad (39)$$

where $[L_{AA}]$ and $[L_{VV}]$ are lower triangular matrices. Shifting techniques are applied to keep the factorization stable [3].

The greatest contributor to the computational costs of a single PCG iteration is given by a matrix-times-vector multiplication of the type

$$\begin{bmatrix} M_{AA} & M_{AV} \\ M_{VA} & M_{VV} \end{bmatrix} \cdot \begin{bmatrix} \vec{p}_A \\ \vec{p}_V \end{bmatrix} = \begin{bmatrix} \vec{q}_A \\ \vec{q}_V \end{bmatrix}. \quad (40)$$

With (35), this operation is performed more efficiently as

$$\vec{p}_E = \vec{p}_A + [G] \cdot \vec{p}_V, \quad (41)$$

$$\vec{q}_A = [M_{EE}] \cdot \vec{p}_E, \quad (42)$$

$$\vec{q}_V = [G]^T \cdot \vec{q}_A. \quad (43)$$

Compared to the underlying \vec{E} scheme, the overhead is just $2K$ additions plus $2K$ subtractions.

The following two observations help improve the PCG algorithm even further:

1) The solution vector in terms of the electric field, \vec{x}_E , can be updated efficiently in each iteration step without evaluating the potentials. The explicit calculation of \vec{x}_A and \vec{x}_V is therefore unnecessary.

2) The residual of the underlying \vec{E} scheme, \vec{r}_E , is readily available throughout the iteration. Due to (33), we simply have $\vec{r}_E = \vec{r}_A$. We use \vec{r}_E for the termination criterion.

Since the resulting ICCG algorithm is now written in terms of $[M_{EE}]$, \vec{x}_E , and \vec{r}_E , the simplified $\vec{A} - V$ method may even be regarded as an \vec{E} scheme with a very specific preconditioner employing an explicit basis for gradient fields. We propose the following implementation:

- Input: equation set $[M_{EE}]$, \vec{r}_E ; preconditioner $[G]$, $[L_A]$, $[L_V]$; termination criterion ϵ .
- Initialization: $\vec{r}_V = [G]^T \cdot \vec{r}_E$; $\vec{x}_E = \vec{p}_A = \vec{0}$, $\vec{p}_V = \vec{0}$; $\rho_{old} = 1.0$
- Iteration:

solve $[L_A][L_A]^T \vec{z}_A = \vec{r}_E$; solve $[L_V][L_V]^T \vec{z}_V = \vec{r}_v$;

$\rho := \vec{r}_E \cdot \vec{z}_A + \vec{r}_V \cdot \vec{z}_V$; $\beta := \rho / \rho_{old}$; $\rho_{old} := \rho$;

$\vec{p}_A := \vec{z}_A + \beta \vec{p}_A$; $\vec{p}_V := \vec{z}_V + \beta \vec{p}_V$; $\vec{p}_E := \vec{p}_A + [G] \cdot \vec{p}_V$;

$\vec{q}_A := [M_{EE}] \cdot \vec{p}_E$; $\vec{q}_V := [G]^T \cdot \vec{q}_A$;

$\alpha := \rho / (\vec{p}_V \cdot \vec{q}_V + \vec{p}_A \cdot \vec{q}_A)$;

$\vec{x}_E := \vec{x}_E + \alpha \vec{p}_E$; $\vec{r}_E := \vec{r}_E - \alpha \vec{q}_A$; $\vec{r}_V := \vec{r}_V - \alpha \vec{q}_V$;

If $(\|\vec{r}_E\| < \epsilon)$ exit.

- Output: solution \vec{x}_E , residual \vec{r}_E .

IV. NUMERICAL RESULTS

To verify the efficiency of our approach, we have applied the \vec{E} formulation, the basic $\vec{A} - V$ scheme, and the new formulation to the following test examples:

A) two cascaded waveguide (WG) bends,

B) a microwave patch antenna.

The finite element models were realized as tetrahedra meshes with perfectly matched layers (PMLs) [13] [14] as port truncations and first order absorbing boundary conditions (ABCs) at interfaces to outer space. The norm of the relative residual in the PCG termination criterion was set to 10^{-4} .

Figs. 1 and 2 show the geometries and results for *Examples A* and *B*, respectively. Since the solutions obtained by the original and modified $\vec{A} - V$ formulations differ in the last few digits only, no separate data are presented. Comparisons of the program runtimes are given in Figs. 3 and 4. Computational parameters such as matrix sizes, iteration counts, and memory

requirements, are listed in TABLE I. It can be seen that the new approach achieves the shortest solution times and requires significantly less storage than the original $\vec{A} - V$ method. Typical memory savings are in the order of 40 %.

In a second set of experiments, we kept the operating frequency constant and varied the mesh density. Figure 3 illustrates the dependence of CPU time on the number of unknowns for the bended waveguide at 9.5 GHz and the patch antenna at 7.5 GHz: Compared to the basic $\vec{A} - V$ scheme, the simplified formulation improves runtimes by a constant factor $k \approx 0.6$. As expected, the computational complexity of both implementations is the same.

V. CONCLUSION

A fast TVFEM solver has been presented. The proposed formalism combines the simplicity and modest memory requirements of the field formulation with the superior numerical convergence of the ungauged vector potential method. Several numerical examples are given to validate the efficiency of the suggested approach. The new method has been presented for edge elements only, but its extension to schemes of higher order appears to be straightforward.

References

- [1] J.F. Lee, D.K. Sun, Z.J. Cendes, "Tangential vector finite elements for electromagnetic field computation," *IEEE Trans. Magn.*, vol. 27, pp. 4032-4035, Sept. 1991.
- [2] I. Bardi, R. Dyczij-Edlinger, O. Biro, K. Preis, "Edge Finite Element Formulations for Waveguides and Cavity Resonators," *eEsi*, pp. 116-121, H. 3, 111.Jg., 1994.

- [3] R. Dyczij-Edlinger and O. Biro, "A Joint Vector and Scalar Potential Formulation for Driven High Frequency Problems Using Hybrid Edge and Nodal Finite Elements," *IEEE Trans. Microwave Theory Tech.*, vol. 44, no. 1, pp. 15-23, Jan. 1996.
- [4] K. Fujiwara, T. Nakata, H. Ohashi, "Improvement of Convergence Characteristic of ICCG Method for the A- ϕ Method Using Edge Elements, " *IEEE Trans. Magn.*, vol. 32, no. 3 pp. 804-807, May 1996.
- [5] R. Albanese and A. Rubinacci, "Solution of three dimensional eddy current problems by integral and differential methods," *IEEE Trans. Magn.*, vol. 24, no. 1, pp 98-101, Jan. 1988
- [6] H. Kanayama, H. Motoyama, K. Endo, and F. Kikuchi, "Three-dimensional magnetostatic analysis using Nedelec's elements," *IEEE Trans. Magn.*, vol. 26, pp. 682-685, Mar. 1990.
- [7] J.B. Manges and Z.J. Cendes, "A Generalized Tree-Cotree Gauge for Magnetic Field Computation," *IEEE Trans. Magn.*, vol. 31, no. 3, pp. 1342-1347, May 1995.
- [8] J. Nedelec, "Mixed finite elements in \mathfrak{R}^3 " *Numer. Math.*, vol. 35, pp. 315-341, 1980.
- [9] A. Bossavit, "Whitney forms: a class of finite elements for three-dimensional computations in electromagnetism," *IEE Proc.*, vol. 135, pt. A, pp. 493-500, Nov. 1988.
- [10] G.H. Golub, C.F. van Loan, *Matrix Computations*, The John Hopkins University Press, Baltimore, 1989.
- [11] E.F. Kaasschieter, "Preconditioned conjugate gradients for solving singular systems," *J. Comput. Appl. Math.* vol. 24, pp. 265-275, 1988.
- [12] Y. Notay, "Incomplete Factorizations of Singular Linear Systems," *BIT*, vol. 29, pp. 682-702, 1989.

- [13] J. P. Berenger, "A Perfectly Matched Layer for the Absorption of Electromagnetic Waves," *J. Comp. Physics*, 114, pp. 185-200, 1994.
- [14] Z. S. Sacks, D. M. Kingsland, R. Lee and J. F. Lee, "A Perfectly Matched Anisotropic Absorber for Use as an Absorbing Boundary Condition," *IEEE Trans. Antennas Propagat.*, vol. 43, pp. 1460-1463, 1995.
- [15] J.M. Reiter, F. Arndt, "Rigorous Analysis of Arbitrarily Shaped H- and E-Plane Discontinuities in Rectangular Waveguides by a Full-Wave Boundary Contour Mode-Matching Method," *IEEE Trans. Microwave Theory Tech.*, vol. 43, no. 4, pp. 796-801, April 1995.
- [16] D.M. Sheen, S.M. Ali, M.D. Abouzahra, J.A. Kong, "Application of the Three-Dimensional Finite-Difference Time-Domain Method to the Analysis of Planar Microstrip Circuits," *IEEE Trans. Microwave Theory Tech.*, vol. 38, no. 7, pp. 849-857, July 1990.

TABLE I: COMPARISON OF DIFFERENT FORMULATIONS

Model	Formulation	Unknowns vector	scalar	Non- zeros	Solver	Iter.	CPU time in sec.	Memory in Mb
Microstrip at 0.2 GHz	modif. $\vec{A} - V$	20094	3852	235675	ICCG	129	59.8	13.3
					DCG	565	138.5	9.1
	orig. $\vec{A} - V$	20094	3852	407317	ICCG	179	210.7	24.6
					DCG	964	342.6	13.7
	\vec{E}	20094	0	202806	ICCG	1576	653.6	12.8
					DCG	6516	1131.5	8.5
WG bends at 9.5 GHz	modif. $\vec{A} - V$	32233	4880	327876	ICCG	180	122.9	21.1
					DCG	962	342.6	13.7
	orig. $\vec{A} - V$	32233	4880	553757	ICCG	244	324.1	33.1
					DCG	1003	536.7	14.4
	\vec{E}	32233	0	289517	ICCG	2604	1661.7	21.8
					DCG	14222	3816.5	11.9
Patch antenna at 7.5 GHz	modif. $\vec{A} - V$	60369	6537	522698	ICCG	1971	2262.7	43.4
					DCG	8166	4710.2	22.6
	orig. $\vec{A} - V$	60369	6537	822191	ICCG	2381	4041.2	52.3
					DCG	8413	6848.2	23.8
	\vec{E}	60369	0	480995	ICCG	13282	14609.4	37.0
					DCG	58007	27380.3	19.9

The iteration counts for the two potential methods were somewhat different, because the original scheme used the total residual $\text{col}(\vec{r}_A, \vec{r}_V)$ as PCG termination criterion, whereas the new one evaluates $\|\vec{r}_E\|$.

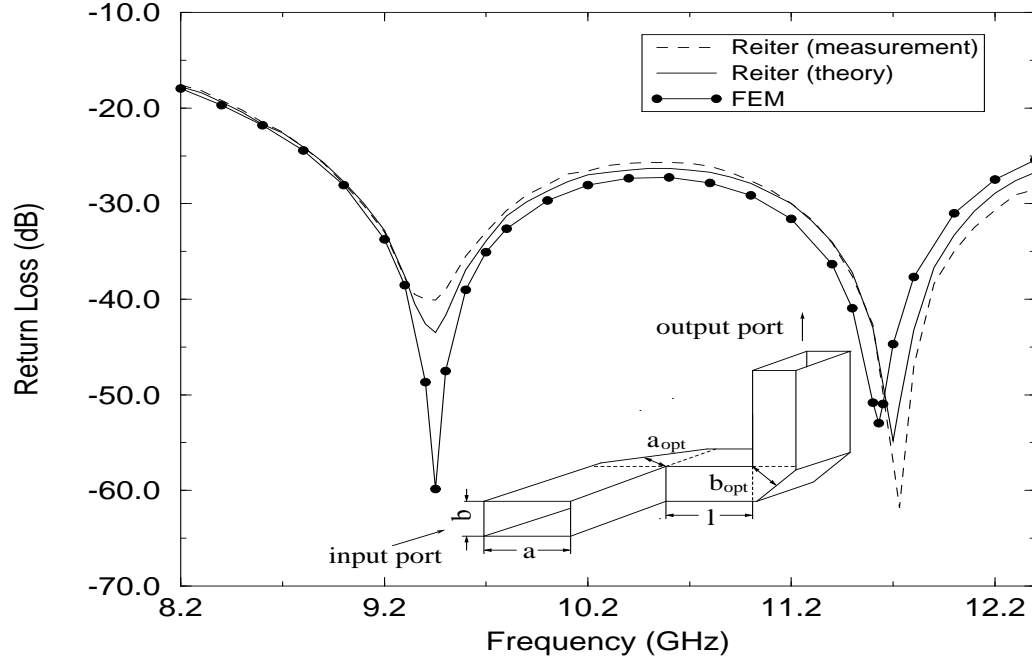


Figure 1: Two cascaded waveguide bends. Dimensions:

$$a = 22.86mm, b = 10.16mm, l = b, a_{opt} = 0.976a, b_{opt} = 0.874b.$$

Reference results taken from Reiter and Arndt [15]

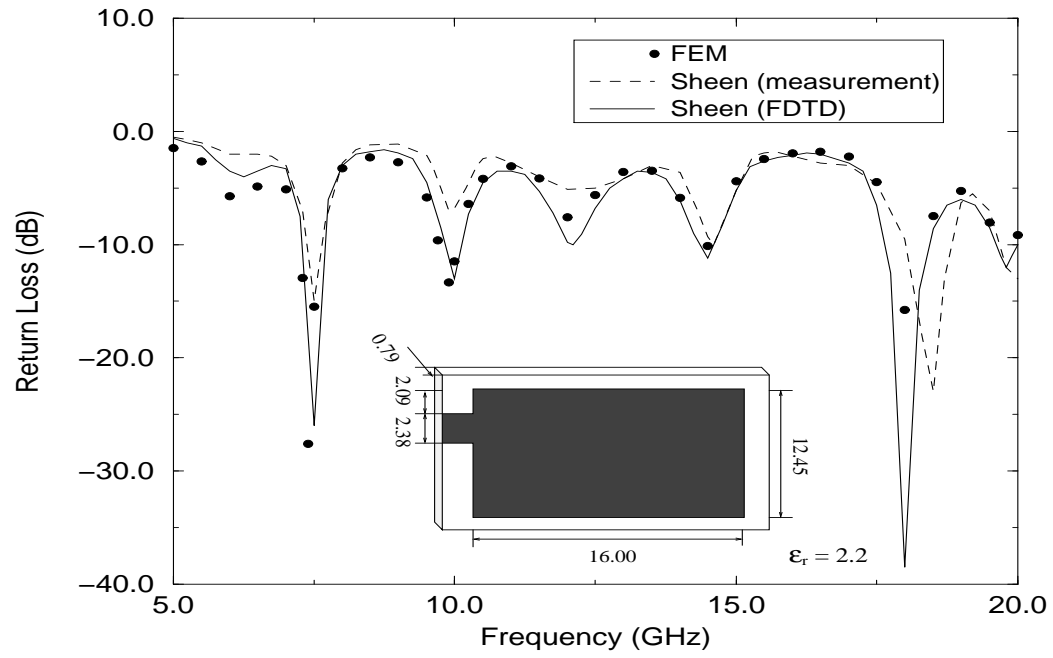


Figure 2: A microwave patch antenna. Reference results taken from Sheen et al. [16]

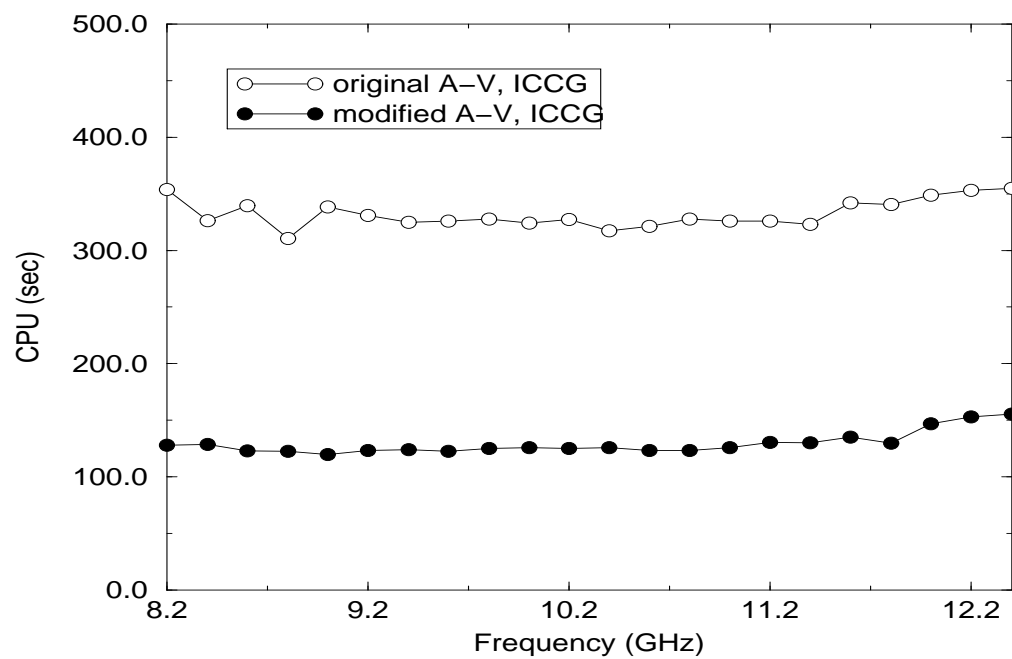


Figure 3: CPU time versus frequency for the waveguide bends.

Solver: ICCG. Workstation: HP 9000/C100, clock speed 120 MHz.

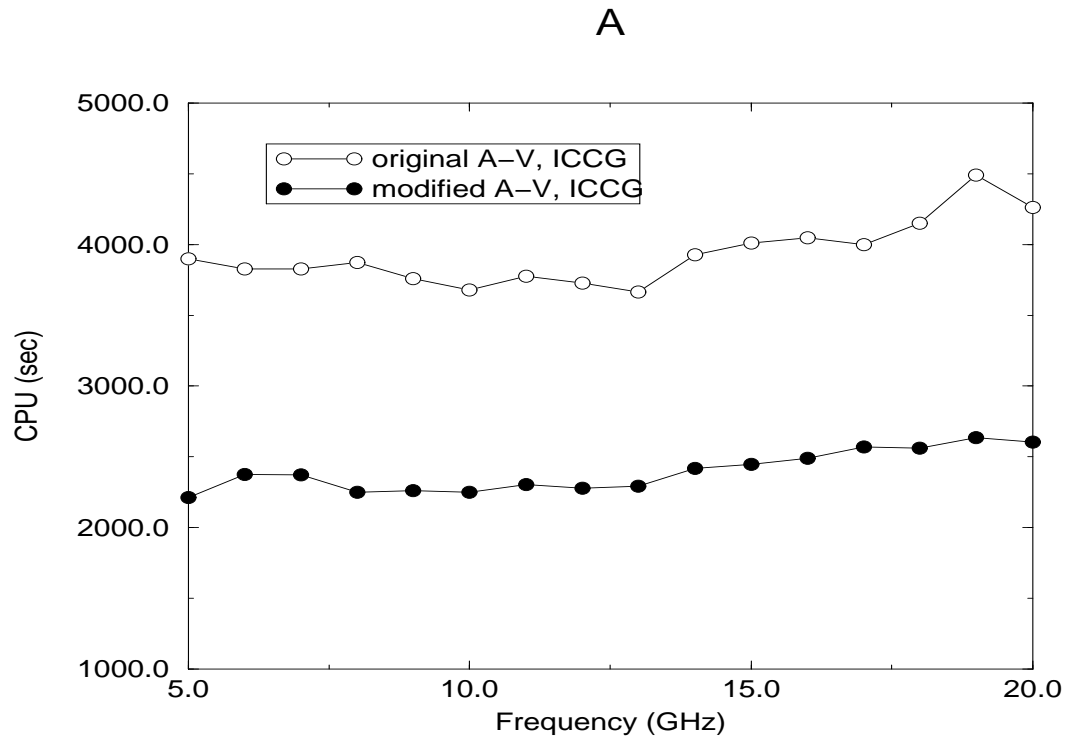


Figure 4: CPU time versus frequency for the microwave patch antenna.

Solver: ICCG. Workstation: HP 9000/C100, clock speed 120 MHz.

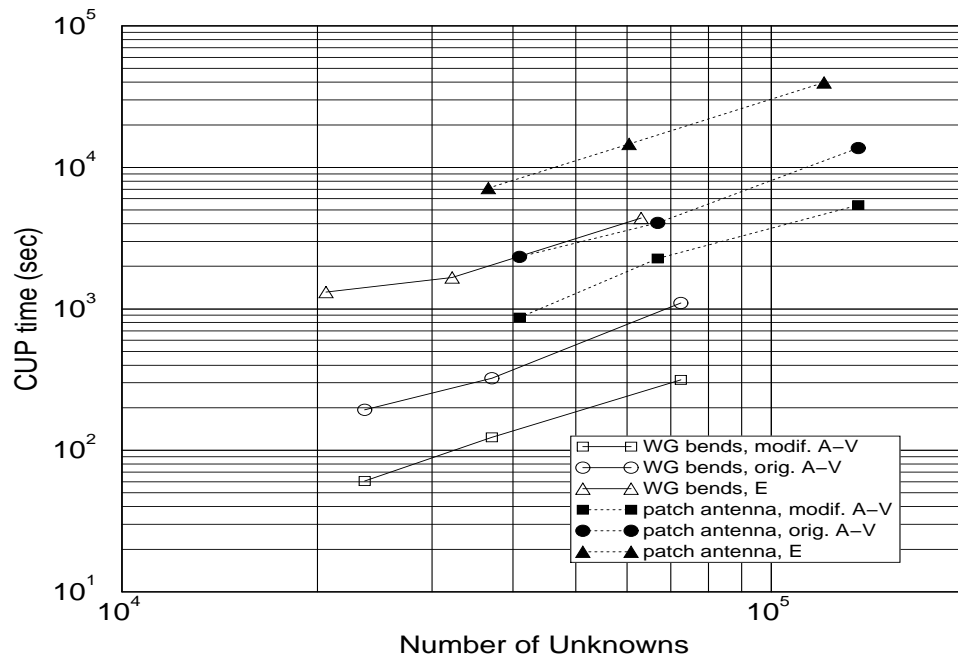


Figure 5: Computational complexity